Progress In Electromagnetics Research M, Vol. 84, 11–20, 2019

A Novel CPW-Fed Planar Monopole Antenna with Broadband Circularly Polarization

Tingting Chen*, Jingjing Zhang, and Weijiang Wang

Abstract—A novel CPW-fed planar printed monopole antenna with broadband circular polarization (CP) characteristic is presented. The proposed antenna consists of a copper coin-shaped patch (CCSP) and an asymmetrical ground plane. To achieve a broadband CP wave, a vertical stub is added to the CCSP to produce orthogonal surface currents for right-hand circular polarization (RHCP). The design of the CCSP greatly increases the impedance bandwidth (IBW) of 89.2% which can cover the whole CP bandwidth of 71% completely. The measured results show that the proposed antenna has not only a broad 3-dB AR bandwidth (ARBW) of 71% (3900 MHz, 3.1–7 GHz) with respect to the CP center frequency 5.8 GHz, but also a wide 10-dB return loss bandwidth of 89.2% (5040 MHz, 2.16–7.2 GHz) centered at 5.65 GHz.

1. INTRODUCTION

For deploying a transmitter and a receiver without causing a polarization mismatch between them, circular polarization is becoming popular in wireless communications to improve system performance, providing better mobility and weather penetration compared to linearly polarized (LP) antennas [1]. Many designs of circularly polarized (CP) patch antennas with single or dual feed structures are proposed by exciting two orthogonal modes with 90° phase difference [2]. Meanwhile, CP antennas with broad bandwidth are needed in modern communication applications to obtain a high data rate and provide high-speed multimedia service [3]. In order to obtain a wide impedance bandwidth and wide axial ratio bandwidth, a variety of printed monopole antenna configurations have been proposed in research papers [4–7], designing an L-shaped monopole slot antenna with a C-shaped feed to realized CP operation [4], placing a power division network between a slot and a monopole for generating circular polarization [5], utilizing two parasitic strips to achieve a broadband CP radiation [6], or protruding a G-shaped parasitic strip into a C-shaped monopole antenna to facilitate wide ARBW [7]. Being fed by CPW-fed structures [8–14], a microstrip antenna can obtain wide operating bandwidth too, and its single metallic layer is better to meet the requirements of low profile and is easier to integrate with the active and monolithic circuits than traditional antennas. By etching modified slots in the ground plane [8–11], designing two orthogonal equal-size patches [12], or adding parasitic strips [13, 14], broadband CPW-fed CP antennas are achieved.

Most of the broadband CPW-fed antennas utilize various parasitic elements or ground planes with slots embedded. In this paper, a novel CCSP with an asymmetrical ground plane is designed to achieve broad impedance and AR bandwidths. The measured performance of the antenna has good agreement with simulated results obtained by Ansoft High Frequency Structure Simulator (HFSS). According to measured results, the -10 dB S_{11} bandwidth is about 89.2%, entirely covering the 3-dB ARBW of 71%. Details of the antenna design procedure are described and analyzed. Several key geometrical parameters are well studied. The proposed antenna can be applied to WLAN and WiMAX communication systems.

Received 19 June 2019, Accepted 1 August 2019, Scheduled 14 August 2019
* Corresponding author: Tingting Chen (ctt_ting@126.com).
The authors are with the College of Electronic Information Engineering, Shandong University of Science and Technology, Qingdao, Shandong 266590, China.

2. ANTENNA DESIGN AND ANALYSIS

2.1. Antenna Configuration

Figure 1 shows the configuration of the proposed CP monopole antenna. The antenna is fed by CPW structure with a feedline of length $L_f = 28\,\text{mm}$, width $W_f = 2\,\text{mm}$, and two identical gaps of widths $g = 0.35\,\text{mm}$. The radiator and ground plane are printed on an FR4 microwave substrate with a thickness of 0.8 mm, relative permittivity of 4.4, and loss tangent of 0.02. By designing the asymmetrical ground plane, the fundamental mode of the antenna can be degenerated into two equally amplitude orthogonal modes with phase quadrature to create a CP mode at higher frequency. In order to excite multiple resonant modes and obtain a wide impedance bandwidth, improvements in extending the top of the rectangular patch to a circle patch with a diameter of D has been made on the basis of the conventional monopole antenna. A key design is etching an inverted L-shaped slot in the middle of the circular patch, which forms the CCSP, greatly increasing the bandwidth of the antenna. Furthermore, a vertical stub is introduced into the monopole structure to excite CP modes at lower frequencies. By tuning the length (L_{stub}) of the stub, CP modes have been merged to get a wide ARBW. The specific dimensions of the proposed antenna are optimized by using HFSS and presented in Table 1.

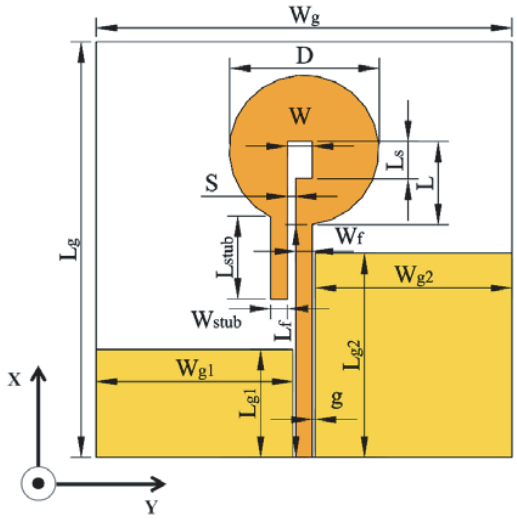

Figure 1. Geometry of the proposed antenna.

Table 1. Geometrical parameters of the proposed antenna (Unit: mm).

Parameter	Value	Parameter	Value	Parameter	Value
W_g	50	D	18	W_{stub}	4.4
L_g	50	W	3	W_f	2
W_{g1}	23.65	L	10	L_f	28
L_{g1}	13	S	1	g	0.35
W_{g2}	23.65	L_s	4.5	h	0.8
L_{g2}	24.6	L_{stub}	10		

2.2. Antenna Design Procedure

In order to explain the design procedure of the proposed antenna, five steps are shown in Figure 2. Prototype Ant.1 is based on the antenna prototype in [14], consisting of only a rectangular patch and a ground plane. In order to achieve CP performance, Ant.2 reduces the length of the left ground plane to

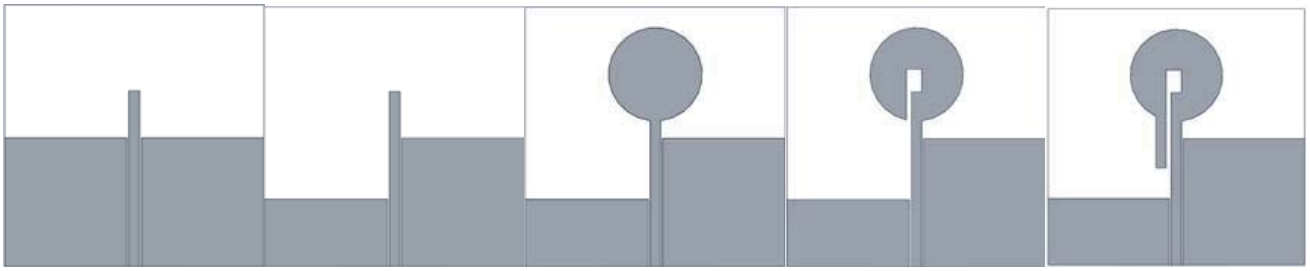

(a) (b) (c) (d) (e)

Figure 2. Five improved prototypes of the CCSP antenna. (a) Ant.1, (b) Ant.2, (c) Ant.3, (d) Ant.4, (e) proposed.

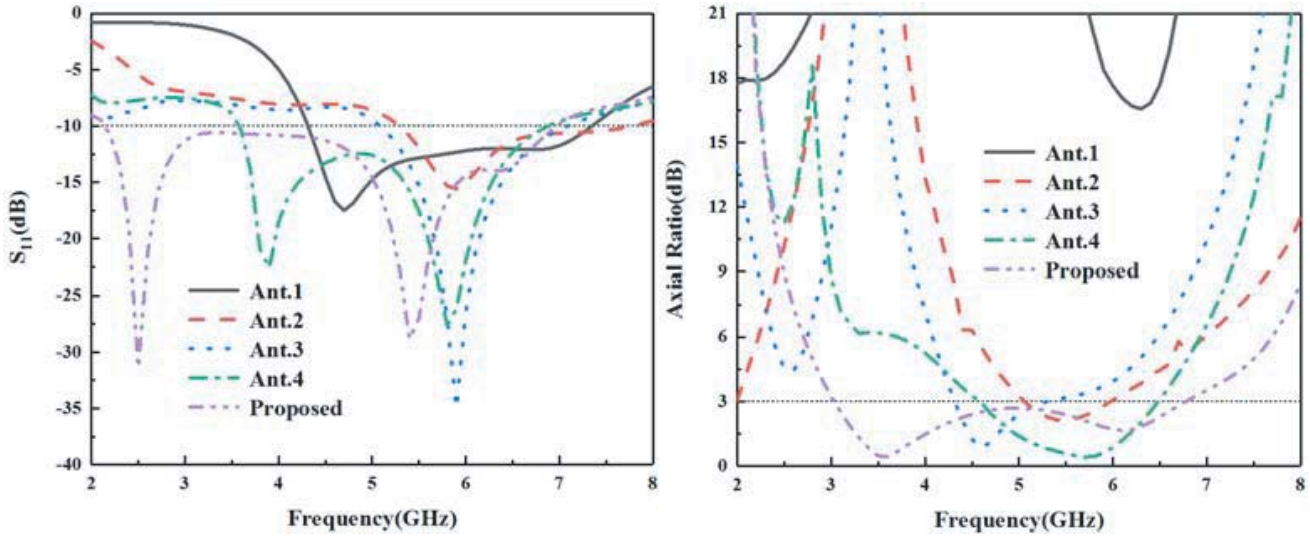

(a) (b)

Figure 3. (a) Simulated S_{11} and (b) axial ratio of Ant.1–4 and proposed.

form an asymmetrical ground plane, which is different from the method of etching a horizontal slot and adding a vertical stub to the ground plane adopted in [13]. According to [15], broadening the top of the rectangular patch can improve impedance matching and obtain wider impedance bandwidth. In this paper, a better impedance matching can be achieved by widening the top of the patch to a circle instead of a traditional rectangle. From the curves of the return loss coefficient and the axial ratio coefficient of Ant.1–4 and proposed antenna shown in Figure 3, it can be seen that Ant.1 does not have the condition of circular polarization. When the ground planes of both sides of the microstrip line is asymmetric, circular polarization can occur at 5.5 GHz. When the top of the patch is widened which is denoted by Ant.3, it can be clearly seen from the red and blue lines of Figure 3(a) that the impedance matching of the antenna is greatly improved. Ant.4 is modified on the basis of Ant.3, and an inverted L-shaped slot is etched in the center of the circular patch to form the CCSP which generates an additional resonance at 3.8 GHz due to coupling. The inner circumference of the CCSP is about a quarter of the wavelength of the free space at a frequency of 3.7 GHz.

$$l = \frac{c}{4f_0} \Rightarrow l = W + L + L_s + (W - S) \tag{1}$$

Accordingly, length l in this design is approximately 20 mm. The modification of the L-shaped slot not only makes the antenna have dual-frequency characteristics, widens the bandwidth by nearly double, but also reduces the axial ratio of the 3–4 GHz band. Finally, a vertical stub is added to the CCSP to

form the proposed antenna, which greatly increases the IBW and ARBW. Furthermore, the comparison of the IBW and ARBW of Ant.1-4 and the proposed antenna is shown in Table 2. It can be seen that the final proposed antenna has a greatly wide IBW and ARBW.

Since the size change of L-shaped slot will affect the size and position of the stub, it is necessary to first determine the size of L-shaped slot of CCSP without stub to facilitate the parameter analysis of the stub in the later section of the paper. Since the addition of the L-shaped slot mainly causes Ant.4 to resonate at low frequencies, the change in length and width of the slot mainly affects the lower frequency of the antenna and has little effect on the higher frequency, as shown in Figures 4 and 5. Figure 4(a) illustrates that with the increased value of L from 8.5 to 10.5 mm, the lower resonant frequency is left shifted, and IBW is increased. As shown in Figure 4(b), AR is reduced at lower frequency, and ARBW is increased due to the disturbance of the electric current on the CCSP. An increase in the width W of

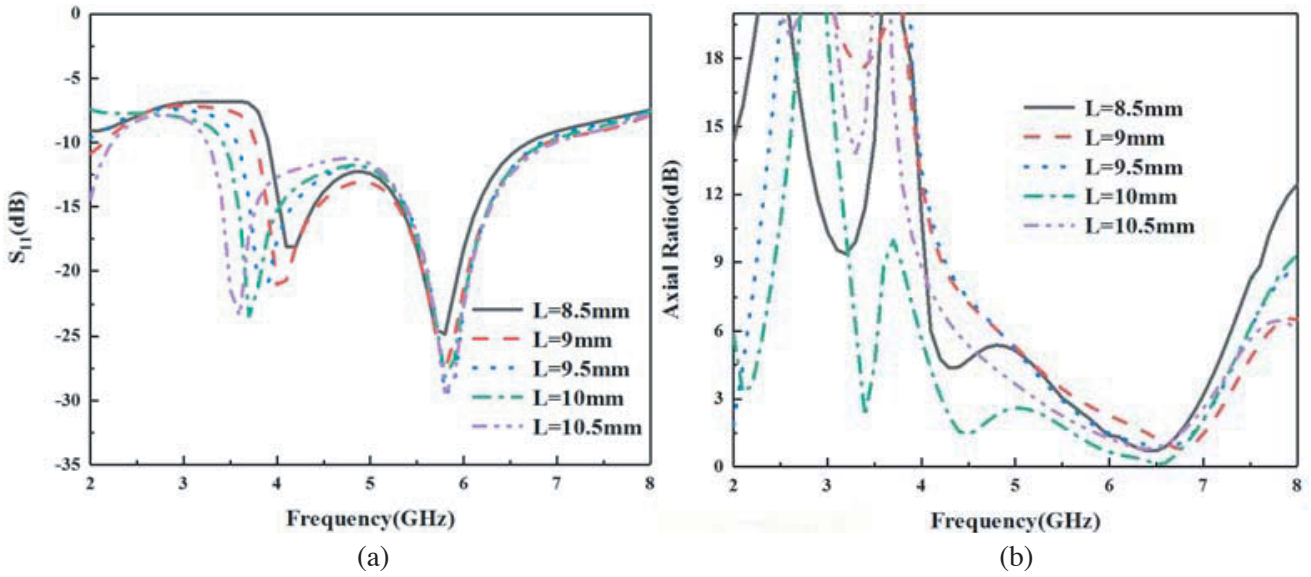

Figure 4. Effects of L on Ant.4 performances (a) S_{11} and (b) axial ratio.

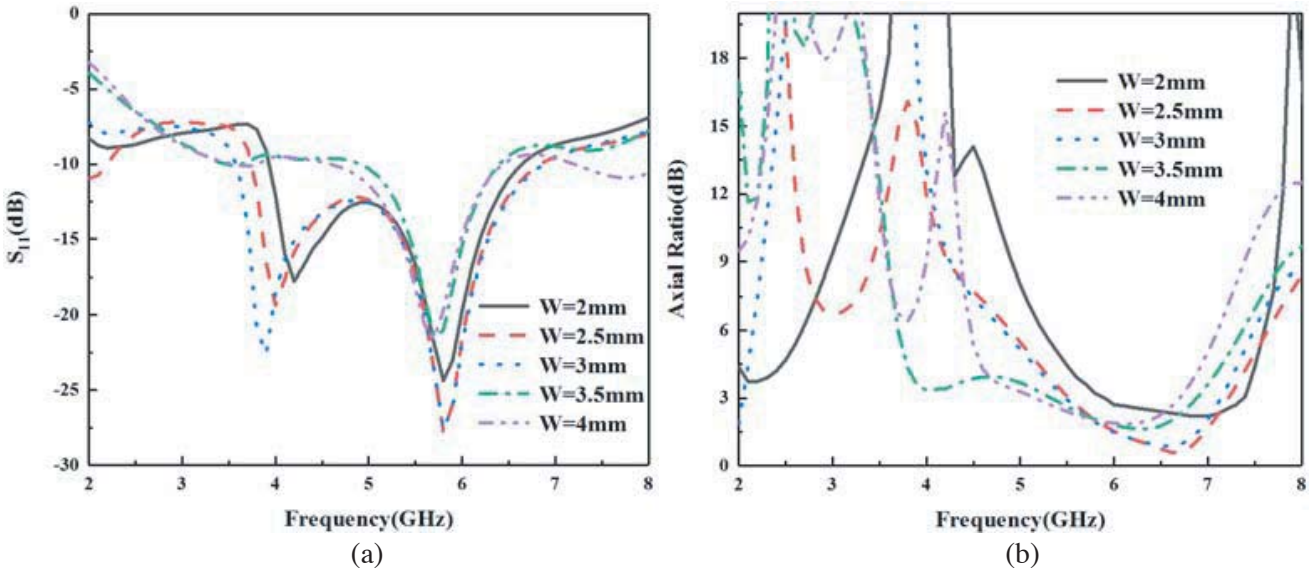

Figure 5. Effects of W on Ant.4 performances (a) S_{11} and (b) axial ratio.

Table 2. Antennas performances of constructed prototypes.

	IBW (MHz)	ARBW (MHz)
Ant.1	2900	No
Ant.2	2400	800
Ant.3	1900	1100
Ant.4	3350	1900
Proposed	4820	3800

the slot also causes the lower frequency to move downward, but when $W > 3$ mm, the first resonance disappears due to the weakening of the coupling effect, as depicted in Figure 5(a). W has little effect on AR operation of 5.8 GHz when $W > 2.5$ mm. According to this analysis, the best values of L and W are selected as 10 mm and 3 mm, respectively, to form the CCSP without the stub.

2.3. Parametric Studies

To understand the effects of various parameters on S_{11} and AR performance, different parametric studies are conducted on the antenna using Ansoft HFSS simulation software, which utilizes 3D full wave finite element method (FEM). At the time of parametric analysis, other parameters are kept as constant at their final optimized value.

2.3.1. Effects of the Diameter of the Circular Patch on the Proposed Antenna (D)

Figure 6 displays S_{11} and AR curves for various D. It is observed that by increasing D from 16 to 20 mm, the resonant frequency is slightly left shifted. When D is larger than 18 mm, the impedance matching at around 3.3 GHz deteriorates, and the IBW becomes narrower. Figure 6(b) illustrates that with the increased value of D from 16 to 18 mm, the lower center frequency of AR is lift shifted, and the AR value of the entire band decreases. When $D = 18$ mm, the lower and higher CP resonant frequency modes are close to each other, and combination of these modes can greatly enhance the AR bandwidth. When $D > 18$ mm, the CP resonant frequency is seen to right shifted. Finally, D is chosen as 18 mm for getting widest ARBW.

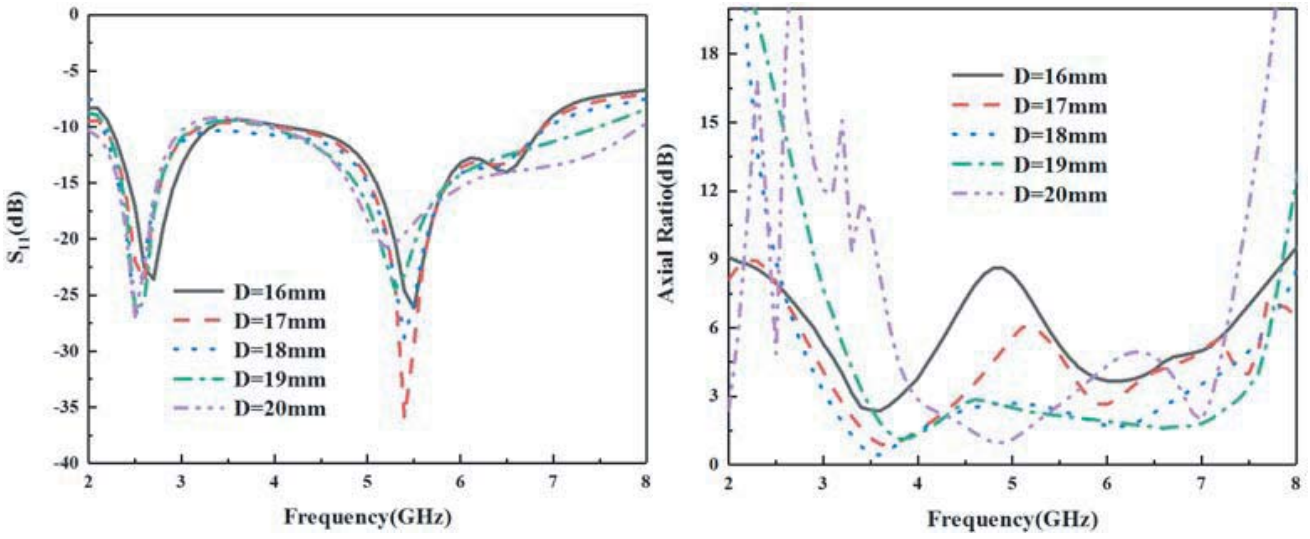

Figure 6. Effects of D on antenna performances (a) S_{11} and (b) axial ratio.

2.3.2. Effects of the Length of the Stub on the Proposed Antenna (L_{stub})

A vertical stub is added to Ant.4 to form the final antenna. In Figure 7, the length of the stub L_{stub} is investigated to find its effect on the antenna performance. It is noted that it has a great impact on IBW and ARBW performance of the proposed antenna. As the length of the stub is increased, the resonant frequency is left shifted, and IBW is increased. AR performance is found sensitive for the variation of L_{stub}. It can be found that the lower CP resonant mode is right shifted, and AR decreases due to the addition of the stub. These modes are merged as the length of the stub increases, which can greatly enhance the ARBW of the proposed antenna, shown in Figure 7(b). Finally, L_{stub} is chosen as 10 mm to achieve maximum IBW and 3 dB ARBW.

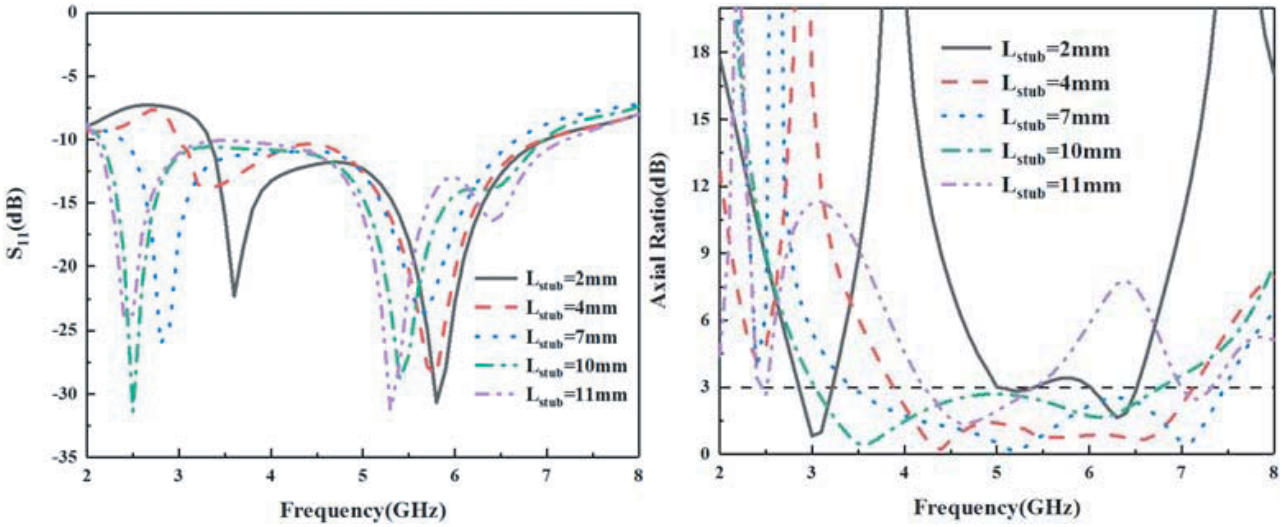

Figure 7. Effects of L_{stub} on proposed antenna performances (a) S_{11} and (b) axial ratio.

2.4. CP Mechanism

The asymmetrical ground plane perturbs the surface current distributions and produces a CP wave at higher frequency of 5.5 GHz. The CCSP disturbs the current distribution of the antenna and produces J_X and J_Y with unequal magnitudes. J_X and J_Y are the x- and y-directed electric currents, which can generate electric fields E_X and E_Y for the far-field radiation. However, CP requires orthogonally directed horizontal and vertical electric fields or same directed electric and magnetic fields with equal magnitude and 90° phase difference. A stub is incorporated in Ant.4 to balance the magnitude of horizontal and vertical electric field to make them equal with 90° phase difference for CP wave generation. With the addition of the stub, electric current path is increased in the antenna structure. Therefore, the resonant frequencies of the antenna are shifted to the left, and a CP mode is generated at lower frequency of 3.5 GHz. Surface current distribution of the proposed CCSP antenna is further studied for illustrating the CP mechanism. In Figure 8(a), it can be seen that the vertical components in the ground plane are in the opposite direction. Hence, under the far-field condition, the radiation in the vertical direction is relatively weak due to the power cancelation. Thus, the predominant surface current flow on the ground plane is in $-y$-direction at 0°. Similarly for CCSP, the main current is in the x-direction. At a later time instant with a 90° phase lagging, a predominant x directed current flow is observed on the ground plane, while a principal $-y$ directed current flow is observed on the CCSP. At 180°, predominant electric current is along $-x$- and y-directions, respectively. It can be observed from Figures 8(b) and (d), the magnitude of the surface current distribution is the same in both cases but oppositely directed for 90° and 270°. This indicates that the direction of rotation of the current is counterclockwise, which means that the proposed antenna provides RHCP wave in the boresight direction and LHCP wave in the opposite direction.

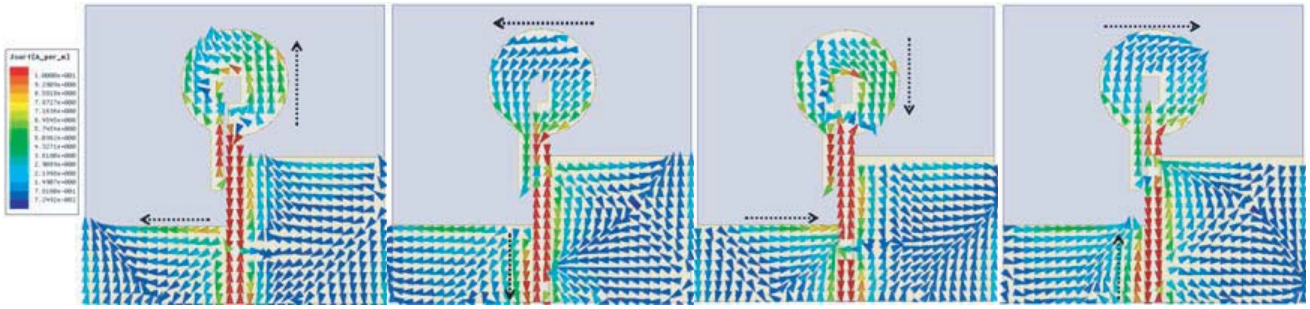

Figure 8. Surface current distributions for the CP center frequency at 5.8 GHz with phase of 0°, 90°, 180°, and 270°. (a) Phase = 0°, (b) Phase = 90°, (c) Phase = 180°, (d) Phase = 270°.

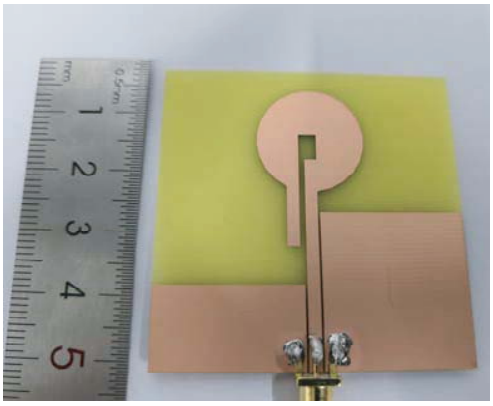

Figure 9. Photograph of proposed antenna.

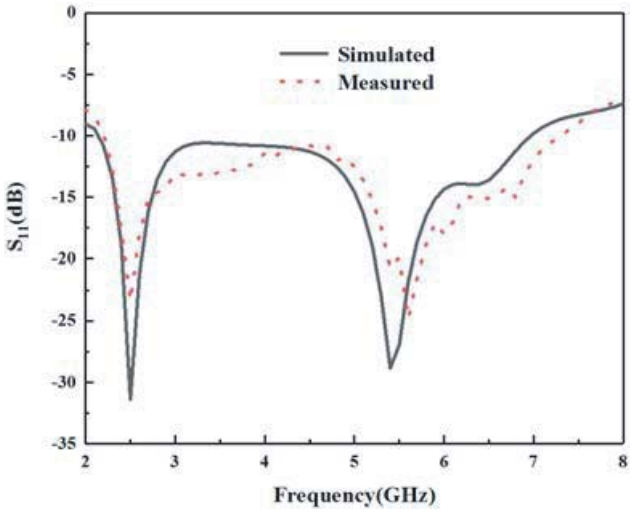

Figure 10. Simulated and measured S_{11}.

Table 3. Comparison of the proposed antenna with referred antennas.

Ref.	Size (mm^2)	CP center frequency (GHz)	IBW (%)	ARBW (%)
[4]	7×70	1.75	30	23
[5]	103×186	2	51	30
[6]	55×50	3.4	88	64.7
[7]	32×30	5.8	62.9	53.9
[11]	25×24	3.375	56.9	47.8
[12]	20×21.8	5.05	36.41	10.3
[14]	24×25	5.9	76.9	44.9
Proposed	50×50	5.8	89.2	71

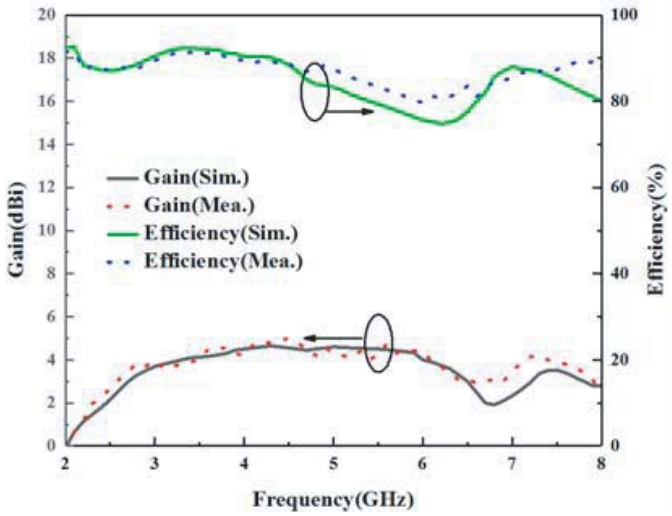

Figure 11. Simulated and measured gain and efficiency.

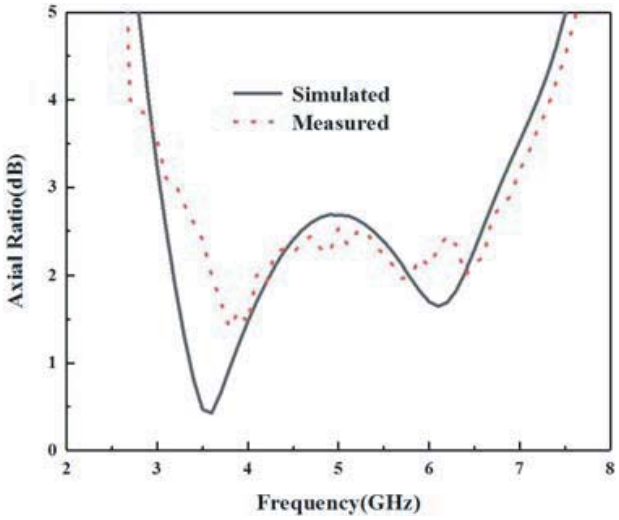

Figure 12. Simulated and measured AR.

3. RESULTS

A prototype with the optimized dimensions in Table 1 has been fabricated, as shown in Figure 9, and measured to verify the simulated results. The simulated and measured S_{11} performances of the proposed antenna are depicted in Figure 10. It can be observed that the simulated and measured IBWs are 87.6% centered around 5.5 GHz (2.15–6.97 GHz) and 89.2% centered around 5.65 GHz (2.16–7.2 GHz), respectively. For measuring the gain of the fabricated antenna, one LP antenna is used in two orientations, and the partial gains, G_{TV} and G_{TH}, are combined to yield the total gains as [16]

$$GT = 10\log(G_{TV} + G_{TH})\,[\text{dBi}] \tag{2}$$

Figure 11 depicts the simulated and measured gains and efficiencies over the entire working frequency band. It can be seen that the measured gain is between 2 and 5 dBi, and the measured efficiency is higher than 80%. ARBW is observed as 69.1% (3–6.8 GHz) and 71% (3.1–7 GHz) from simulated and measured results, respectively, in Figure 12. The normalized radiation patterns of the proposed antenna in xz ($\varphi = 0°$) and yz ($\varphi = 90°$) plane are shown in Figures 13(a) and (b) at 3.5 GHz and 5.5 GHz, respectively. From the bidirectional property of the proposed antenna, it can be observed that the

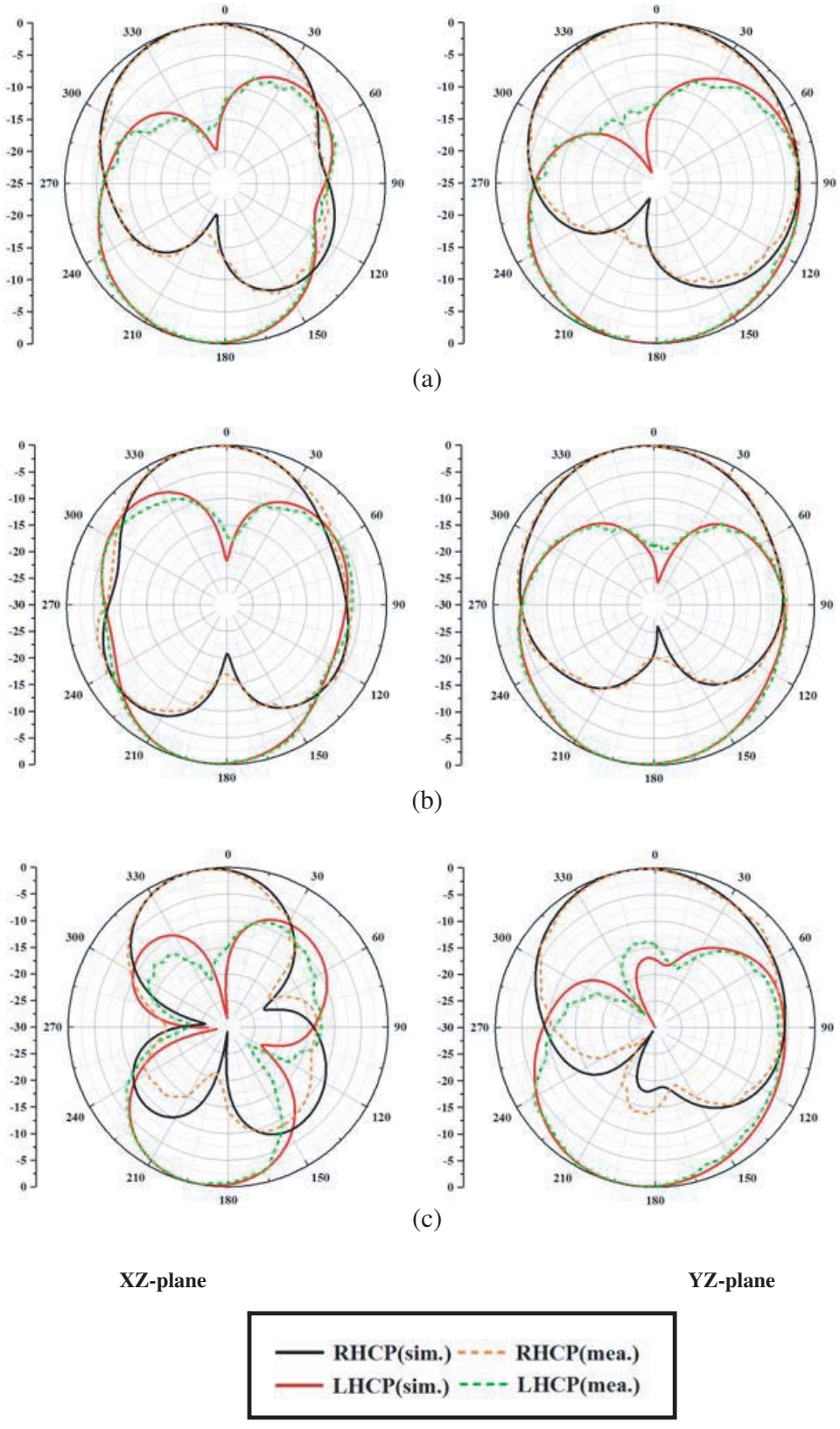

Figure 13. Simulated and measured patterns of the proposed antenna at (a) 3.5 GHz, (b) 4.4 GHz and (c) 5.5 GHz.

antenna radiates RHCP wave in the boresight direction ($+z$) and LHCP wave in opposite direction ($-z$) as shown in Figure 13.

Comparisons between the proposed antenna and previous antennas are shown in Table 3, which includes antenna size, IBW, and 3 dB ARBW. It illustrates that the proposed antenna has the superiority of the widest IBW and widest ARBW with a quite simple structure.

4. CONCLUSION

A novel broadband CPW-fed monopole antenna with wide ARBW has been proposed, fabricated, and tested in this communication. The proposed antenna comprises an asymmetric ground plane and a CCSP. By appropriately adding a vertical stub to the CCSP, the AR and impedance bandwidths of the antenna are greatly enhanced. The proposed antenna can be a better candidate for WLAN, WiMAX, and other broadband communication systems owing to its structural simplicity, low production cost, and broad bandwidth.

REFERENCES

1. Sze, J. Y. and C. C. Chang, "Circularly polarized square slot antenna with a pair of inverted-L grounded strips," *IEEE Antennas Wireless Propag. Lett.*, Vol. 7, 149–151, 2008.
2. Ferrero, F., C. Luxey, G. Jacquemod, et al., "Dual-band circularly polarized microstrip antenna for satellite applications," *IEEE Antennas Wireless Propag. Lett.*, Vol. 4, 13–15, 2005.
3. Counselman, III, C. C., "Multipath-rejecting GPS antennas," *Proc. IEEE*, Vol. 87, 86–91, 1999.
4. Mousavi, P., B. Miners, and O. Basir, "Wideband L-shaped circular polarized monopole slot antenna," *IEEE Antennas Wireless Propag. Lett.*, Vol. 9, 822–825, 2010.
5. Kumar, T. and A. R. Harish, "Broadband circularly polarized printed slot-monopole antenna," *IEEE Antennas Wireless Propag. Lett.*, Vol. 12, 1531–1534, 2013.
6. Ding, K., C. Gao, and Y. Wu, "A broadband circularly polarized printed monopole antenna with parasitic strips," *IEEE Antennas Wireless Propag. Lett.*, Vol. 16, 2509–2516, 2017.
7. Midya, M., S. Bhattacharjee, and M. Mitra, "Broadband circularly polarized planar monopole antenna with G-shaped parasitic strip," *IEEE Antennas Wireless Propag. Lett.*, Vol. 18, 581–585, 2019.
8. Wang, C. J. and C. M. Lin, "A CPW-fed slot antenna for multiple wireless communication systems," *IEEE Antennas Wireless Propag. Lett.*, Vol. 11, 620–623, 2012.
9. Jan, J. Y., C. Y. Pan, K. Y. Chiu, and H. M. Chen, "Broadband CPW-fed circularly-polarized slot antenna with an open slot," *IEEE Trans. Antennas Propag.*, Vol. 61, 1418–1422, 2013.
10. Li, G. H., H. Q. Zhai, T. Li, and C. H. Liang, "CPW-fed S-shaped slot antenna for broadband circular polarization," *IEEE Antennas Wireless Propag. Lett.*, Vol. 12, 619–622, 2013.
11. Chen, Q., H. Zhang, L.-C. Yang, B. Xue, and X.-L. Min, "Broadband CPW-fed circularly polarized planar monopole antenna with inverted-L strip and asymmetric ground plane for WLAN application," *Progress In Electromagnetics Research C*, Vol. 74, 91–100, 2017.
12. Midya, M., S. Bhattacharjee, and M. Mitra, "Compact CPW-fed circularly polarized antenna for WLAN application," *Progress In Electromagnetics Research M*, Vol. 67, 65–73, 2018.
13. Pourahmadazar, J., C. H. Ghobadi, J. Nourinia, et al., "Broadband CPW-fed circularly polarized square slot antenna with inverted-L strips for UWB applications," *IEEE Antennas Wireless Propag. Lett.*, Vol. 10, 369–372, 2011.
14. Zhang, L., Y. C. Jiao, Y. Ding, et al., "CPW-fed broadband circularly polarized planar monopole antenna with improved ground-plane structure," *IEEE Trans. Antennas Propag.*, Vol. 61, 4824–4828, 2013.
15. Jan, J. Y. and C. Y. Hsiang, "Wideband CPW-fed slot antenna for DCS, PCS, 3G and bluetooth bands," *IEE Electron. Lett.*, Vol. 42, 1377–1378, 2006.
16. Stutzman, W. L. and G. A. Thiele, *Antenna Theory and Design*, 2nd Edition, Wiley, New York, 1998.